A Study on the Development of a 3D Digital Twin Model for the Safety Diagnosis of Natural Heritage

Chaewon Kim [1], Jaeyong Lee [2], Choongsik Kim [3]

[1] Dept. of Heritage Science and Technology Studies, Graduate School of Korea Heritage, Korea National University of Heritage, Republic of Korea - ja90722@naver.com
[2] Dept. of Traditional Landscape Architecture, Korea National University of Heritage, Republic of Korea - leejaeyong82@knuh.ac.kr
[3] Dept. of Heritage Science and Technology Studies, Graduate School of Korea Heritage, Korea National University of Heritage, Republic of Korea - kimch@knuh.ac.kr

Keywords: Wind load, Damage, Decay, Monitoring, Finite Element Analysis (FEA).

Abstract

The objective of this study was to quantitatively diagnose the structural stability of old-giant-trees by establishing a finite element analysis (FEA) method. This study selected four protected trees in Buyeo-gun, South Korea, in consideration of field applicability, including tree growth conditions and data acquisition environment, and conducted structural diagnosis. The study was conducted in the order of creating a 3D analysis model, setting conditions for FEA, and diagnosing structural stability. The main results of this study are as follows. First, this study established a method for building 3D shapes of crown, trunk, and decay models using 3D scanning and SoT. Second, this study proposed conditions for FEA, including the calculation of tree weight and wind load according to the shape of the tree and parameters of tree properties. Third, the FEA results of a tree with trunk decay revealed that the probability of trunk breakage was not high even under strong winds (70m/s) during typhoons. Nevertheless, this study confirmed that decay would affect the internal stress distribution and safety factor and cause structural vulnerability. The importance of this study is that it proposed an FEA method reflecting the shape of the old-giant-tree and its internal decay. However, future experiments need to address the shortcomings of high parameter values in this study (the highest wind penetration rate in the crown).

1. Introduction

Old-giant-trees are very valuable from various angles, including historical, biological, and academic perspectives. However, they are more susceptible to damage from external forces such as high winds and heavy snowfall than younger trees because their age makes them less vigorous and weakens their structural functions (Costello and Berry, 1991). Particularly, a recent escalation in the magnitude and frequency of weather disasters has increased the damage to old-giant-trees. Broken branches and treefalls are the most common damage types to old-giant-trees due to extreme weather events (Korea Heritage Service, 2023). For example, Typhoon Lingling toppled down the Needle Fir near Haksadae Pavilion of Haeinsa Temple, Hapcheon, (a natural monument) in 2019, and Typhoon Khanun tore off the main root of the Multi-stem Pine of Dokdong-ri, Gumi, causing it to fall in 2023 (National Research Institute of Cultural Heritage, 2023). As physical damage to old-giant-trees is increasing, it is critical to identify potential decay before it occurs and take appropriate countermeasures.

Many recent studies quantitatively diagnosed the structural stability of trees by using finite element analysis (FEA) (Kim et al., 2021; National Research Institute of Cultural Heritage, 2023). These analytical studies mainly focused on the maximum deflection zone or stress generation due to external forces. However, they did not consider decay, which is an important factor in analyzing structural stability or used estimated decay. Decay was considered in only a few studies. The objective of this study was to quantitatively diagnose the structural stability of old-giant-trees by building a three-dimensional analysis model and establishing an FEA method.

2. Materials and Methods

2.1 Subject of Study

The subject of the study was Zelkova (Zelkova serrata(Thunb.) Makino), which accounts for a large portion of Korea's natural heritage trees. This study selected four Zelkova (A, B, C, and D) in Buyeo-gun, which is in the central region of South Korea, considering the tree shape and history of tree surgery (Table 1). They were old-giant-trees with an age of more than 300 years and representative tree characteristics. Tree A grew erect, and its crown developed to the northwest. No trace of tree surgery or cavities was found by visual tree assessment (VTA). The trunk of Tree B was tilted to the west, and its crown developed to the east. There was a 2.1-meter-high open decay on the east side that touched soil surface. The step of Tree C tilted to the east, and at approximately 2m in height, the trunk first forked to the north and west. No decay was identified by VTA. Tree D grew erect, with primary branching at 2.2m in height. The crown was divided into two parts by the forked branches. No decay was found by VTA.

2.2 Methodology

The study was conducted in the order of acquiring tree growth data, creating a 3D analysis model, and diagnosing structural stability by using FEA.

Tree shape data and decay data were acquired for the 3D analysis model in the tree growth data acquisition stage. The former was acquired by using Geo Slam ZEB-GO, a 3D scanning device, and the latter was obtained by using PiCUS 3 Sonic Tomography (SoT, Argus Electronic GmbH, Rostock, Germany). The decay data of the trunk was acquired at five different heights at 30cm

https://doi.org/10.5194/isprs-archives-XLVIII-M-9-2025-1735-2025

Classification	A	B	C	D
Tree height (m)	7	17	17	8
Diameter at breast height (m)	4.3	4.7	3.3	4.3
Tree shape				
Location	685-3 Sin-ri, Gyuam-myeon, Buyeo-gun	70-4 Jinbyeon-ri, Gyuam-myeon, Buyeo-gun	35-3 Samyong-ri, Nam-myeon, Buyeo-gun	439 Osu-ri, Gyuam-myeon, Buyeo-gun

Table 1. Subject of study.

intervals to diagnose the overall structural stability of the tree. The data from 3D scanning and SoT were converted into separate three-dimensional models using GeomagicWrap and Rhino7.0, respectively.
The structural stability of the old-giant-trees was analyzed using the FEA method. FEA is a way of finding approximate solutions to differential or partial differential equations for complex structures that cannot be solved by analytical methods. FEA was carried out using Ansys 2023R2.

3. Results

3.1 Building FEA Models

The 3D shape information of the trunk and crown was acquired using 3D scanning (Figure 1). The acquired point cloud was separated into trunk and crown by using Cloudcompare's Colorimetric Segmenter function. The crown part was created using Rhino 7.0 and Grasshopper programs. Section lines that reflected the plane shape by height were created based on the points cloud of the crown. Then, a 3D mesh was built based on the section lines. The trunk part was created using the Geomagic Wrap program, and it was a 3D mesh based on the points cloud. The decay model was also a 3D mesh, which was built by decay cross sections at the five heights, obtained by SoT, with Rhino 7.0 and Grasshopper. The final trunk model was constructed by subtracting the decay model from the trunk model because decayed areas do not play a structural role, and trees behave like hollow tubes (Mattheck et al., 2014).
Then, an analysis model was created to conduct structural analysis. The structural analysis model consists of elements and nodes, and the accuracy of analysis results depends on the number of elements and nodes. If there are many elements, the error of the approximate solution becomes smaller, and the accuracy of the analysis increases. However, it increases the number of unknowns and equations to be solved, which consequently elevates costs. Therefore, it is needed to examine the quality of the mesh to reduce the cost of the analysis and produce reliable results. Mesh skewness is one of the ways to check the quality of the mesh. It was developed to make the maximum skewness of the analysis mesh 0.95 or less or the average skewness 0.33 or less (Ansys, 2010).

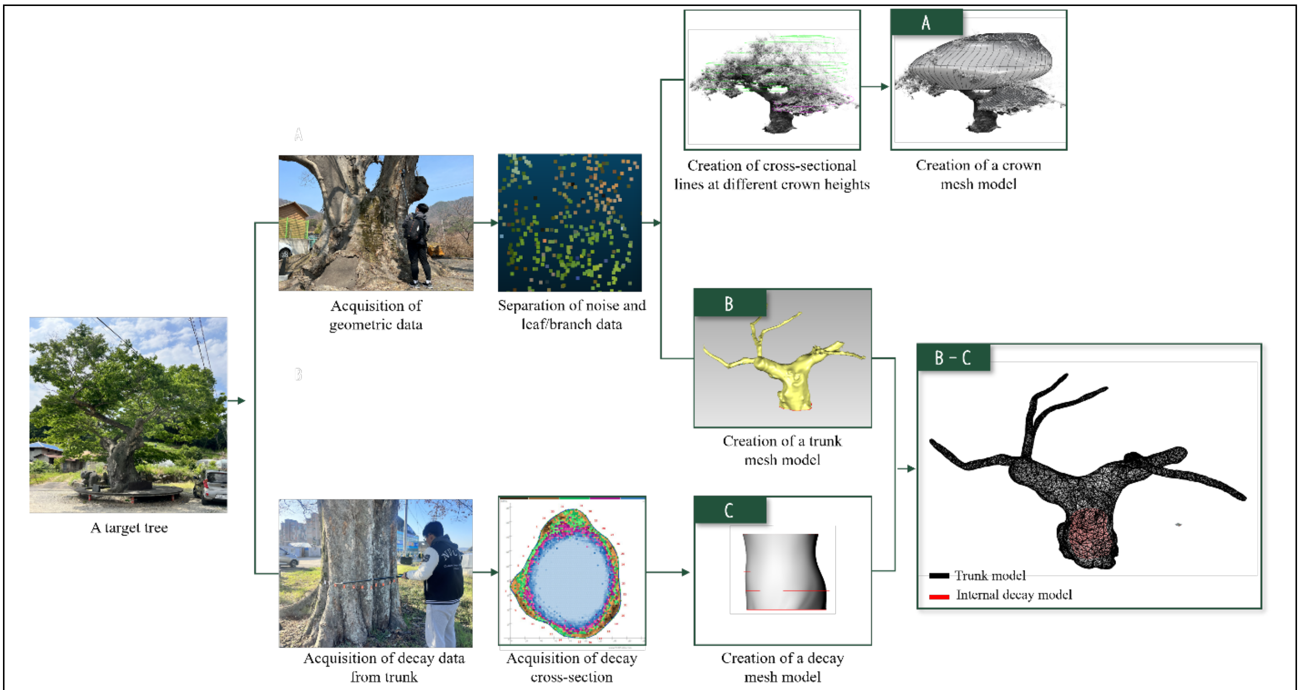

Figure 1. Flow of building a finite element analysis (FEA) model.

3.2 Setting FEA Conditions

Initial conditions were set to diagnose the structural stability of the old-giant-tree (Table 2). Wood is generally regarded as an anisotropic material, but, in the absence of fundamental data regarding anisotropy, the analysis was conducted under the assumption that it is isotropic (Kim, 2020). This study used the experimentally proven mean values of elastic modulus and strength (Ministry of Forestry, Japan, 1973) (Table 3). The specific gravity of Zelkova green lumber was set to 0.85 (Korea Forest Research Institute, 2008).

Type	Elastic modulus	Compression strength	Tensile strength	Flexural strength	Shear strength
Mean	11767.98	49.03	127.49	98.07	12.75
Min	7845.32	34.32	83.36	68.65	7.85

Table 3. Elastic modulus and strength of Zelkova (Ministry of Forestry, Japan, 1973)

It is necessary to set support objects for static structural analysis is necessary, and it depends on the purpose and scope of the analysis. The support conditions were set by assuming that the bottom of the old-giant-tree model was fixed to the ground.
The load was determined on the assumption that the crown's own weight and wind load are applied to the crown's center of gravity (Mayer, 1987). The crown's own weight was calculated using the formula for the weight of landscape trees (Eq. 1) and the weight distribution ratio of trees proposed by Lee (1996) (Table. 4).

$$W = k_1 \pi (\frac{d}{2})^2 H W_0 (1 + P) \qquad (1)$$

where W = weight of the aboveground part
k_1 = shape factor of trunk (typically 0.5)
d = diameter at breast height (m)
H = tree height (m)
W_0= unit wight of trunk
P = ratio for branches and leaves

Leaves	Branch	Trunk	Root	Total (%)
26	17	43	14	100

Table 4. Weight distribution of trees (Lee, 1996)

The wind direction on an old-giant-tree was set to eight directions: east, west, south, north, northeast, northwest, southeast, and southwest. The wind load was calculated using the drag force calculation formula (Eq. 2). Drag force coefficient (C_d) is a dimensionless number used to quantify the resistance or drag force of an object in a fluid environment, such as air or water, and it changes with the area of the object, illumination, and the density, temperature, and velocity of the fluid. Since the density and temperature of the fluid, the area of the object, and illumination were not considered in this study, the drag force coefficient could be defined as a function of wind speed. This study calculated it by interpolating the drag force coefficients for different wind speeds (0.43 (10 m/s), 0.26 (20 m/s), and 0.20 (30 m/s)) according to the wind speed to consider the change with wind speed (Gerhart, 2017). Since the drag force coefficient tends to converge with increasing wind speed, the wind load was calculated by using a drag force coefficient of 0.20 at 30m/s wind speed (Gerhart, 2017; Kim et al., 2020). The loaded area (A) was calculated by the projected area of the old-giant-tree's crown

	A	B	C	D
Tree volume (㎥)	5.05	6.12	3.95	4.58
Decay volume (㎥)	0.83	2.28	0.32	1.45
Own weight (kg)	3,214	3,172	2,042	1,666
Max skewness	0.91	0.90	0.98	0.97
Mean skewness	0.24	0.24	0.23	0.23
Crown	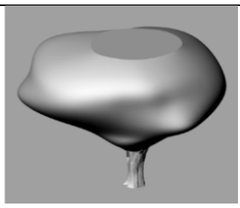	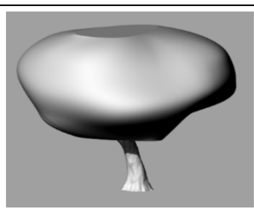	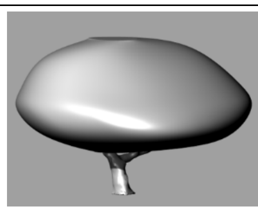	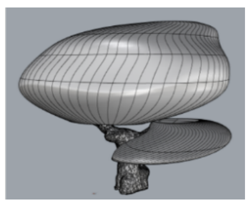
Trunk	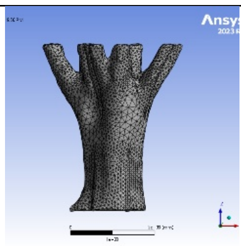	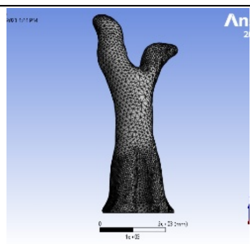	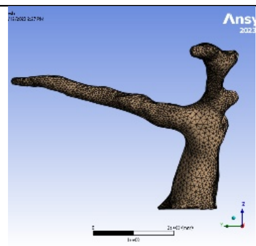	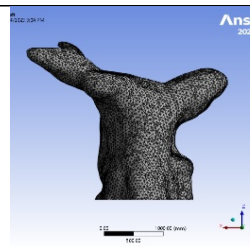
Decay	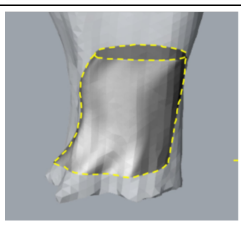	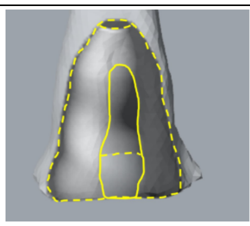	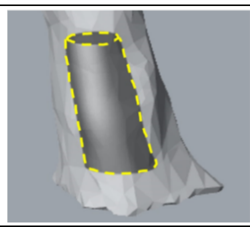	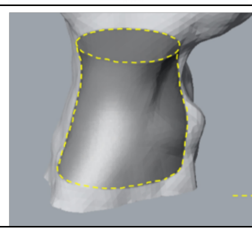

Table 2. Shape information of analysis models.

according to the wind direction, and the penetration ratio of the crown was set to zero for a conservative stability evaluation. The wind speed (v) was set to be uniformly distributed regardless of height, and the density of the fluid (ρ_{air}) was set to 1.184, which is the density of the atmosphere.

$$F_{wind} = \frac{1}{2} C_d A \rho_{air} v^2 \qquad (2)$$

where F_{wind} = drag force calculation formula
C_d = drag force coefficient
A = loaded area
v = wind speed
ρ_{air} = density of fluid

Wind loads on trees were calculated for eight wind directions at various wind speeds (30–70m/s). All four trees exhibited a proportional increase in wind load with increasing wind speed. The wind load on Tree A was similar across all wind directions. At a wind speed of 70m/s, the wind load was approximately 50kN. The wind load on Tree B did not vary by wind direction, except when the wind blew from the west.

Due to its high crown volume and large projected area, wind load could exceed 70kN when wind speed reached 70m/s. Tree C exhibited that the wind load due to south or southwest wind was lower than that due to other wind directions. The crown of Tree D consisted of two parts, and its projected area was smaller than that of other trees. The calculated wind load of the south wind was lower than that of other wind directions at all wind speeds. Except for the south wind, there is no meaningful difference in wind load based on wind speed.

When wind load is applied to trees, moments caused by wind load and moments caused by tree weight occur (Mayer, 1987). Structural failure occurs when the stress generated within the tree due to moments by wind and tree weight exceeds the tree's strength. The structural stability of old-giant trees can be evaluated using the safety factor. The safety factor is calculated by dividing the tree's yield strength by the maximum stress (von-Mises stress) (Eq. 3). Although trees are well-known materials for analysis, the safety factor of 4.5 proposed by Mattheck et al. (1993) was set as the criterion for judgment because structural analysis was conducted under uncertain environmental and stress conditions.

$$\text{safety factor} = \frac{\textit{yield strength}}{\textit{the maximum stress (von-Mises stress)}} \qquad (3)$$

3.3 Diagnosis of Tree Structural Stability using the FEA Method

Stress occurrence and safety factors of the trees were evaluated by setting wind speeds to 70m/s for the eight directions. The FEA results of Tree A showed that five locations (Points 1, 2, 3, 4, and 5) were the maximum stress and critical failure points for wind directions (Table 5). All critical failure points were located within the decayed areas of the trees. Stress was lowest (3.82 MPa) at Point 1 on the south side of the tree under north winds with the highest safety factor (12.83). This could be attributed to the fact that the cross-sectional area of sound wood on the southern side was larger than that on other directions because the decayed area developed toward the northwest direction. The maximum stress and lowest safety factor were derived at Point 4 on the west side of the tree under east, southeast, and northwest winds. Under east and southeast winds, internal stress was the highest (7.44 and 7.06MPa, respectively), and the safety factor was the lowest (6.59 and 6.95, respectively). This phenomenon could be attributed to the development of the decayed area in the northwest direction. Under northwest winds, the stress and safety factor of Point 4 was 4.59MPa and 10.68, respectively. At this location, the magnitude of the stress was different from that under east and southeast winds possibly because when northwesterly winds blew, the stress caused by wind load was offset by the stress caused by the tree’s own weight due to the development of the crown to the northwest. Although the lowest safety factor (6.59) was observed at 70m/s east wind, it was higher than the safety factor of 4.5, the criterion for tree breakage. Therefore, it was judged that the probability of breakage even under strong winds

<table>
<tr><th>Points</th><th>Wind direction</th><th>Maximum stress (MPa)</th><th>Safety factor</th></tr>
<tr><td>1</td><td>N</td><td>3.82</td><td>12.83</td></tr>
<tr><td rowspan="2">2</td><td>NE</td><td>6.36</td><td>7.71</td></tr>
<tr><td>SW</td><td>5.03</td><td>9.75</td></tr>
<tr><td rowspan="3">3</td><td>E</td><td>7.44</td><td>6.59</td></tr>
<tr><td>SE</td><td>7.06</td><td>6.95</td></tr>
<tr><td>NW</td><td>4.59</td><td>10.68</td></tr>
<tr><td>4</td><td>S</td><td>4.90</td><td>10.01</td></tr>
<tr><td>5</td><td>W</td><td>5.07</td><td>9.67</td></tr>
<tr><td rowspan="2">Stress points</td><td>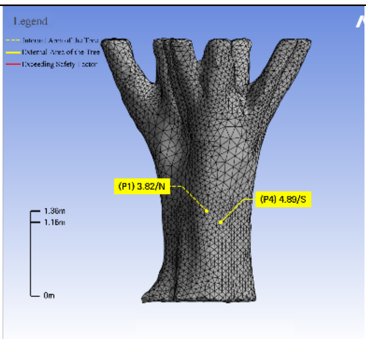
</td><td>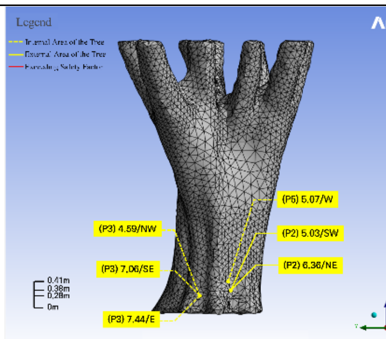
</td><td>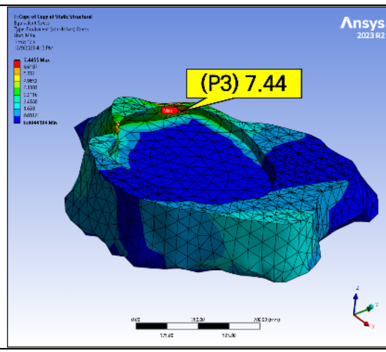
</td></tr>
<tr><td>Maximum stress location (south side view)</td><td>Maximum stress location (west side view)</td><td>Critical failure point</td></tr>
</table>

Table 5. When the wind speed is 70m/s, the maximum stress and safety factor of Tree A for each wind direction

was very low. However, since the safety factor tends to decrease as wind speed increases, observing the decayed area would be important.

In Tree B, there were five (Points 1, 2, 3, 4, and 5) maximum stress and critical failure points by direction (Table 6). Point 3 had the highest stresses of 5.39 MPa and 5.3 MPa and the lowest safety factors of 9.10 and 9.25 under the east and west winds, respectively. Under the east wind, the tree's own weight and wind load generated tensile stress on the east side of the trunk where the opening existed and compressive stress on the west side. Under the west wind, the tree's own weight and wind load caused compressive stress at the opening and tensile stress on the west side of the trunk. It seems that large stresses were generated because the stress distribution caused by the tree's own weight and wind load was similar under the east and west winds. Under the south and southwest winds, although Point 4 at the ground surface had a large cross section of sound wood, the length of the moment arm from the center of gravity of the crown to Point 4 was long. As a result, the stresses were large (4.95 and 5.02MPa). Under the northwest and southeast winds, Point 5 of the trunk showed the lowest stress (3.88MPa) and the highest safety factor (12.6). The locations with the maximum stress and the minimum safety factor suggested that the location of the decay opening affected the stability of trees. However, even under 70m/s east winds, the safety factor was 9.10, indicating that the tree was structurally very stable.

In Tree C, Points 1 and 2 were identified as the maximum stress and critical failure points (Table 7). These points were the north and west branches, both of which were distant from the decayed area. Maximum stresses were found at Point 1, a branch on the north side, under the north, southeast, south, southwest, and northwest winds. Among them, the largest maximum stress was 11.38MPa, and the safety factor was 4.31 under the south wind, suggesting the possibility of breaking. This could be because gravity and wind load are added under the south wind. Under the northeast, east, and west winds, the maximum stress occurred at Point 2 on the west branch. Although the branch on the west side developed better, the stress was greater under the west wind than under the east wind. This is because the stress caused by the east wind was offset by the stress caused by the tree's own weight due to the well- developed branch on the east.

Four maximum stress and critical failure points (Points 1, 2, 3, and 4) were identified for Tree D (Table 8). The highest stress occurred mostly in the areas with thin sound wood, around the decayed area. This is because the cross-section changes abruptly as the thickness of the sound wood gets thinner, which is prone to concentrating the stress. The maximum stress occurred inside the tree under the south wind, and the maximum stress occurred outside the tree under other wind directions. The maximum stress was found at Point 1 point under the north, northwest, and southeast winds. The smallest stress (1.15 MPa) occurred at Point 1 under the north wind because the cross-section of the sound wood was thick in this direction. The difference in compressive stress could make the stress at Point 1 under the northwest wind (2.73MPa) higher than under the southeast wind (2.35 MPa). The maximum stress was found at Point 2 under the west, southwest, and northeast winds due to the relatively thin sound wood in the section where the compressive stress occurred and the uneven shape of the section. The safety factor analysis results revealed that it was close to the maximum safety factor (15) in most wind directions, except for southwest and west winds. It could be because of a smaller wind load due to the lower height and smaller projected area of the tree.

4. Conclusions

The objective of this study was to present a structural stability diagnosis method for old-giant-trees with internal decay. To achieve this objective, this study also examined the creation of an analytical model, the calculation of wind load and tree weight, and the setting of variables for FEA. This study selected four trees from the protected trees growing in Buyeo-gun for creating 3D analysis data and model the decayed area to derive results that could be used in the field. This study calculated the internal stresses and safety factors generated in eight directions by using Ansys, an FEA program. The FEA results showed that even under strong winds (70 m/s) during typhoons, the damage due to a snapped trunk was not likely to occur. It was found that if there

Points	Wind direction	Maximum stress (MPa)	Safety factor
1	N	4.77	10.27
2	NE	4.92	9.96
3	E	5.39	9.10
	W	5.30	9.25
4	SW	5.02	9.77
	S	4.95	9.91
5	SE	3.88	12.62
	NW	3.88	12.64
Stress points		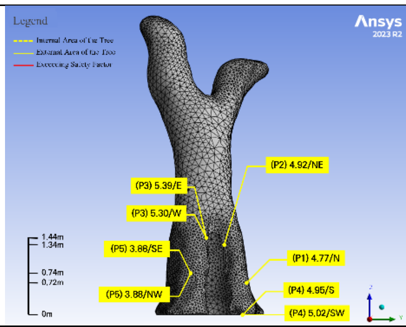	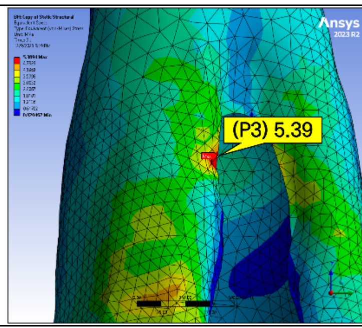
		Maximum stress location (east side view)	Critical failure point

Table 6. When the wind speed is 70m/s, the maximum stress and safety factor of Tree B for each wind direction.

Points	Wind direction	Maximum stress (MPa)	Safety factor
1	S	11.38	4.31
	SW	9.53	5.15
	N	9.48	5.17
	SE	8.59	5.71
	NW	7.63	6.42
2	W	10.20	4.81
	E	10.14	4.83
	NE	8.83	5.55
Stress points	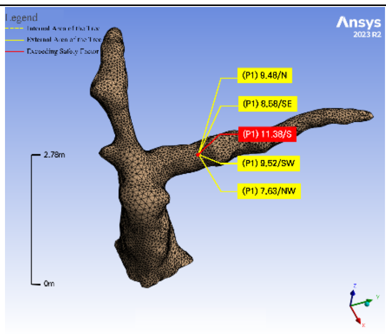	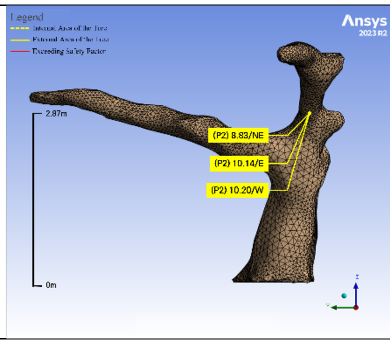	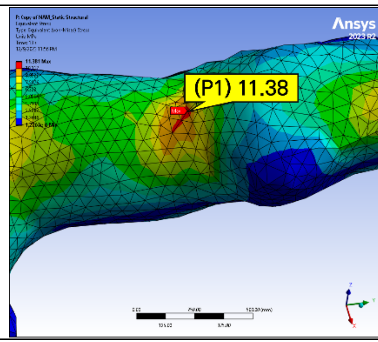
	Maximum stress location (east side view)	Maximum stress location (west side view)	Critical failure point

Table 7. When the wind speed is 70m/s, the maximum stress and safety factor of Tree C for each wind direction.

Points	Wind direction	Maximum stress (MPa)	Safety factor
A	N	1.15	15.00
	SE	2.35	15.00
	NW	2.73	15.00
B	W	3.98	12.31
	SW	3.79	12.94
	NE	2.61	15.00
C	E	3.05	15.00
D	S	2.08	15.00
Stress points	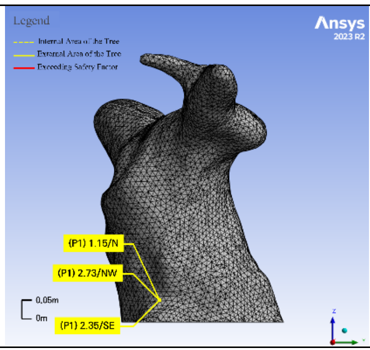	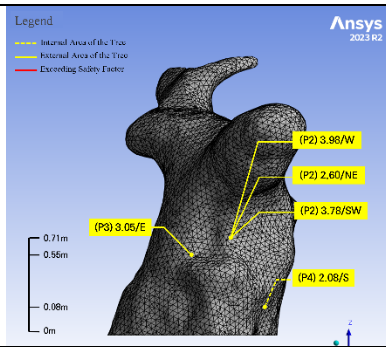	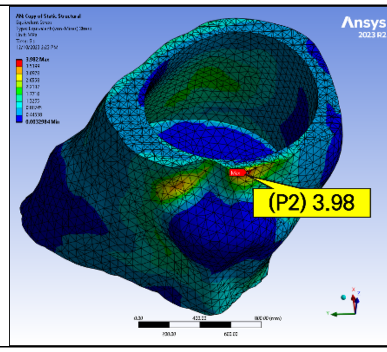
	Maximum stress location (east side view)	Maximum stress location (west side view)	Critical failure point

Table 8. When the wind speed is 70m/s, the maximum stress and safety factor of Tree C for each wind direction.

was some sound wood, the wind load was offset by the tree’s own weight, which secured structural stability. However, it was confirmed that the decayed area of the tree was a structural weakness and a factor that could cause other parts to fail. When trees had low safety factors, indicating the possibility of breakage, lateral branches rather than the trunk were mechanically vulnerable.

It is a meaningful achievement that this study could diagnose the structural stability of trees by using FEA, prepare measures against strong winds, and identify targets and points that requires attention. This study used the maximum crown weight and penetration rate to apply the results to the field due to the lack of experiments and research on trees, and future studies need to address this shortcoming. Nevertheless, it is meaningful to construct shapes of old-giant-trees and propose a structural stability diagnosis method for the old-giant-tree including cavities.

References

Ansys, 2010. Ansys Fluent User’s Guide 13.

Costello, L. R., Berry, A. M., 1991. The California tree failure report program: An overview. J. Arboric., 17(9), 250-255.

Gerhart, P. M., Gerhart, A. L., Hochstein, J. I., 2017. Munson's Fluid Mechanics. John Wiley & Sons, USA.

Jung, Y., Lee, J. Y., 2024. Finite element analysis study on the structural stability of old trees. J. Korean Tradit. Landsc. Archit., 42(3), 42-50.

Kim, Y., Rahardjo, H., Tsen-Tieng, D. L., 2020. Stability analysis of laterally loaded trees based on tree-root-soil interaction. Urban For. Urban Green., 49, 126639. doi.org/10.1016/j.ufug.2020.126639.

Kim, Y., Rahardjo, H., Tsen-Tieng, D. L., 2021. Mechanical behavior of trees with structural defects under lateral load: A numerical modeling approach. Urban For. Urban Green., 59, 126987. doi.org/10.1016/j.ufug.2021.126987.

Korea Heritage Service, 2023. Disaster occurrence statistics and safety management manual for national heritage.

Lee, K. J., 1996. Forest Ecology. Seoul: Hyangmunsa.

Mayer, H., 1987. Wind-induced tree sways. Trees, 1, 195-206.

Ministry of Forestry, Japan, 1973. Handbook of Wood Industry. Maruzen Publishing.

National Research Institute of Cultural Heritage, 2023. Precision structural stability diagnosis of old Zelkova trees for natural disaster response.